

GENERATION OF DISSIPATION-GRAVITY WAVES DURING THERMAL CONVECTION
IN A STRATIFIED MEDIUM

A. V. Kistovich and Yu. D. Chashechkin

UDC 532.516:536.25

In the present article we identify a special class of wave motions, called dissipation-gravity waves (DGWs), on the basis of an asymptotic analysis of the equations for free convection over a localized heat source. We obtain a steady-state solution in the limit $t \rightarrow \infty$, calculate the wavelength and direction of propagation, and determine the nature of the particle motion. We compare the results with data from experiments, in which this type of wave motion was regarded as zero-frequency internal waves [1-3].

The structure and properties of free convective flows over a localized heat source in a stably stratified medium have been subjected to extensive investigation both theoretically [4, 5] and experimentally [1, 2, 6]. The flow pattern formed upon actuation of a heat source in a medium initially at rest depends on the type of stratification. In a temperature-stratified fluid a convective plume mushrooms upward about its axis at the neutral buoyancy level [7]. The flow pattern over a heat source in a medium with salinity stratification is more complex and includes not only main buoyant plume per se, but also a system of vortex cells if the power of the source exceeds a critical value, along with a system of transient internal waves [1, 2, 6, 8].

As an illustration, Fig. 1 shows a motion picture shadowgraph of free convective flow over a warm heating element (a vertical cylinder of height 0.01 m and diameter 0.008 m containing a resistance heater) in a medium with a constant salinity gradient, a stratification

scale $\Lambda_S = \left| \frac{1}{\rho_0(z)} \frac{d\rho_0(z)}{dz} \right|^{-1} = 56$ m, and a buoyancy period $T_b = 2\pi\sqrt{\Lambda_S/g} = 15$ sec, where $\rho_0(z) =$

$\rho_0[S_0(z)]$ is the density, $S_0(z)$ is the salinity, z is the coordinate along the vertical axis, and g is the free-fall acceleration. The power input is $P = 1$ W, and the heating duration is 30 min. Energy is released uniformly over the surface of the cylinder. The shadowgraph was obtained by the conventional technique using a vertical slit and a flat Foucault knife edge at the focus; the variations of the optical density are proportional to the fluctuations of the horizontal component of the refractive index and the density, which are linearly related for solutions of sodium chloride in water [9].

The structure of the convective thermoconcentration flow does not depend on the type of localized heat source [6]. The main structural elements of the flow are shown in Fig. 2. The released heat is concentrated in a bounded zone above the source (region A); this zone radiates a heightwise-regular system of perturbations of the primary salinity field W , i.e., DGWs (or ZFWs [1, 6]), into the surrounding medium. In certain strong convection regimes, ordinary transient internal waves (TIWs) are also radiated from region A into the surrounding medium [3].

Region A contains a heated ascending convective plume 1, a dome of high-salinity liquid 2, and a system of convective vortex cells 3. The high-salinity liquid is entrained in the main plume from the level of the heater. Since heat is transferred more rapidly than salt, the liquid particles begin to heat upon reaching the top and then essentially return to the original level as they cool. When this happens, the primary vortex surrounding the ascending plume closes. The outer shell of this vortex, acting as a secondary heat-releasing element, generates a system of convective cells, in which the liquid flows toward the heated dome and away from it, transferring heat into lower-temperature regions. Significantly, the boundary regions between the main dome and the system of cells (and, accordingly, between the cells) are shear layers, where the velocities of the liquid particles are in opposite directions on opposite sides of the layer with the enhanced density gradient (the liquid flows downward

Moscow. Translated from Zhurnal Prikladnoi Mekhaniki i Tekhnicheskoi Fiziki, No. 3, pp. 49-55, May-June, 1991. Original article submitted January 19, 1988; revision submitted January 5, 1990.

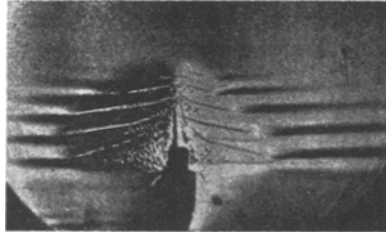


Fig. 1

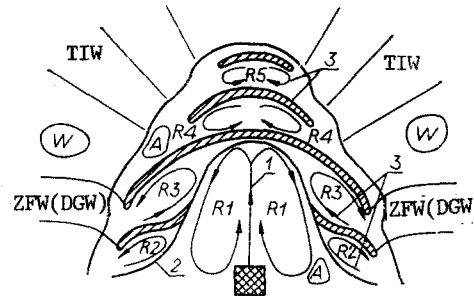


Fig. 2

along the inner surface of the main dome and upward along the outward surface as it is heated in the secondary cells). The liquid flows away from the center of the convection zone in the upper part of the convective cells and toward the center in the lower part. In the zones where the external liquid is entrained, the sharp boundary of the shell gives way to a more diffuse boundary. The pattern of streamlines is indicated by arrows in Fig. 2.

The main distinguishing features of the flows in region A are the high-gradient layers, i.e., the shells of vortex flows, including both the primary vortex R1 surrounding the ascending plume and the smaller-scale vortices R2, ..., R5 forming the regular system of convection cells. In the shadowgraph of Fig. 1 the high-gradient shells are represented by thin elongated oblique light bands on the left side of the convective flow and by dark bands on the right side (the complementary dark bands on the left side and light bands on the right side are not altogether fully developed in the photographs, owing to the limited dynamic range of both the shadow technique itself and the film used to record the effect). The width of the high-contrast intermediate boundary layer corresponds to half the true thickness of the high-gradient shell.

The convective cells proper are outlined by the sharp oblique upper shell and the more diffuse horizontal lower shell. The higher-temperature, higher-salinity liquid in the upper part of the primary vortex R1 and the secondary vortices R2, ..., R5 is unstable against small-scale perturbations and forms thin vertically elongated striae or "salt fingers" [1, 3]. In Fig. 1 the "salt fingers" fill the space between the ascending plume and the dome and continue in the interior of the convective cells in the region adjacent to the main vortex core of the flow.

The system of DGWs is represented by diffuse dark and light bands running from the convection region into the surrounding medium. The optical density along the phase surfaces decreases with increasing distance. Each wave is associated with a corresponding cell. The vertical scale of the spacing between waves is determined by the height of the generating cell, and the angle of inclination of the phase surfaces of the DGWs relative to the horizontal is a maximum in the generation zone at the boundary of the cell and decreases with increasing distance. The flow pattern evolves in the course of heating. In the given regime new cells are formed above the plume (vortex R5 in the diagram of Fig. 2). The stable registration of a new wave begins with the advent of a high-gradient fold, which evinces closure of the vortex motion inside the cell. The slow flows in the heated region A, which correspond to the general light background on the right side and to the darkened background on the left side of Fig. 1, do not radiate DGWs.

The resulting flow pattern is described by the complete system of nonlinear thermodynamic equations. Because of the complexity of their analysis, it is customary to investigate linearized equations describing the flows outside region A [10, 11]. In our specific situation this approach enables us to discern and describe the properties of DGWs, which are recorded outside the convection region in all cellular flow regimes [1, 6].

1. Statement of the Problem. The complete system of equations for thermoconcentration convection in a liquid with stable primary salinity and temperature stratification has the form (see [12], p. 95).

$$\rho(\partial \mathbf{u} / \partial t + (\mathbf{u} \cdot \nabla) \mathbf{u}) = -\nabla p + \nu \rho \Delta \mathbf{u} + \frac{\nu \rho}{3} \nabla (\nabla \cdot \mathbf{u}) + \rho_0 (\beta S' - \alpha T') \mathbf{g},$$

$$\partial S / \partial t + \nabla \cdot (\mathbf{u} S) = k_S \Delta S, \quad \partial T / \partial t + \nabla \cdot (\mathbf{u} T) = \chi \Delta T + Q(R; t),$$

$$\begin{aligned} \partial\rho/\partial t + \nabla \cdot (\mathbf{u}\rho) &= -\alpha\rho_0 Q(R; t), \quad \rho = \rho_0(1 + \beta S - \alpha T), \\ S &= S_0(z) + S', \quad T = T_0(z) + T', \\ S_0(z) &= S_0 \left(1 - \frac{z}{\beta S_0 \Lambda_S}\right), \quad T_0(z) = T_0 \left(1 + \frac{z}{\alpha T_0 \Lambda_T}\right). \end{aligned} \quad (1.1)$$

Here \mathbf{u} is the velocity of the medium; p is the total pressure minus the hydrostatic pressure; S , $S_0(z)$, and S' are the total, stratified, and excess salinities; T , $T_0(z)$, and T' are the total, stratified, and excess temperatures; S_0 and T_0 are the salinity and temperature at the level $z = 0$; ρ is the density of the medium; ρ_0 is the density of the pure liquid; α , β , χ , ν , and k_S are the coefficients of saline and thermal expansion, the thermal diffusivity, the kinematic viscosity, and the salt diffusion coefficient; Λ_S and Λ_T are the scales of salinity and temperature stratification; $Q(R; t)$ is a function describing the heat source, and \mathbf{g} is the gravitational force vector, which is oriented in the negative z -direction. We use the linearized form of the equation of state $\rho(T, S)$ and ignore the compressibility of the medium [12]. The system (1.1) is completely defined; the number of unknowns (\mathbf{u} , ρ , T , S , p) is equal to the number of equations.

The objective of the analysis is to exhibit DGWs and to determine the principal characteristics. As mentioned in the introduction, the system of DGWs exists outside the convection zone, each wave is generated by its own corresponding convection cell, and the DGWs do not interact with each other. These conditions enable us to investigate the properties of a single wave generated by the gradient shell by linearizing the equations and invoking the Boussinesq approximation, whereupon the system (1.1) is reduced to the system

$$\begin{aligned} \partial\mathbf{u}/\partial t &= -\frac{1}{\rho_0} \nabla p + \nu \Delta \mathbf{u} + (\beta S' - \alpha T') \mathbf{g}, \\ \partial S'/\partial t + \nabla \cdot (\mathbf{u} S_0(z)) &= k_S \Delta S', \quad \partial T'/\partial t + \nabla \cdot (\mathbf{u} T_0(z)) = \chi \Delta T' + Q \frac{\delta(z) \delta(r)}{2\pi r} \theta(t), \\ \partial(\beta S' - \alpha T')/\partial t + \nabla \cdot (\mathbf{u}(1 + \beta S_0(z) - \alpha T_0(z))) &= -\alpha Q \frac{\delta(z) \delta(r)}{2\pi r} \theta(t), \end{aligned} \quad (1.2)$$

in which $Q = P/c_p \rho_0$.

The representation of the system (1.2) implies that the outer boundary of the high-gradient shell of the cell is interpreted as a secondary heat source of constant power P , which is actuated at the initial time $t = 0$. This secondary source serves as the reference origin in the coordinate system (r, z) (r is the horizontal, and z is the vertical coordinate). It should be noted that in Eq. (1.2) [as in Eq. (1.1)] the condition $\nabla \cdot \mathbf{u} = 0$ is not used, because it would be inferred from the last three equations of the system (1.2) [and from the corresponding equations (1.1)] that $\Delta(\beta k_S S' - \alpha \chi T') = 0$ in the case of a pure solenoidal velocity field. It follows from this relation, in conjunction with the extinction of the perturbation fields S' and T' at infinity, that $\beta k_S S' = \alpha \chi T'$, which contradicts the experimental results.

The velocity field, which is axisymmetrical, admits the representation [13]

$$\begin{aligned} \mathbf{u} &= \mathbf{v} + \mathbf{w}, \quad \mathbf{v} = -\nabla h, \quad w_r = -\partial\Phi/\partial r, \quad w_z = -\partial\Psi/\partial z, \\ \Delta_r \Phi + \partial^2 \Psi/\partial z^2 &= 0, \quad \Delta_r = r^{-1} \frac{\partial}{\partial r} \left(r \frac{\partial}{\partial r} \right). \end{aligned}$$

Here w_r and w_z are the radial and vertical components of the solenoidal part of the velocity, and h , Φ , and Ψ are unknown functions of the coordinates and time.

We write the components of the total velocity vector in the form

$$u_r = -\partial h/\partial r - \frac{\partial^2 f}{\partial r \partial z}, \quad u_z = -\partial h/\partial z + \Delta_r f, \quad f = \int_0^z \Phi(r, \zeta, t) d\zeta, \quad (1.3)$$

where the unknown function f is related to the familiar stream function by the equation $\psi = r \partial f/\partial r$. The substitution of Eq. (1.3) into (1.2) reduces the basic system to the equations

$$(\partial/\partial t - \chi\Delta)(\partial/\partial t - k_S\Delta)(\partial/\partial t - \nu\Delta)\Delta f - k_S D^2 \Delta \Delta_r f + N^2 \frac{\partial}{\partial t} \Delta_r f = Q(\partial/\partial t - k_S\Delta)\delta(R)\theta(t),$$

$$h = \frac{\chi\nu N^2}{gD^2} \Delta \Delta f + \frac{(1 - \chi/k_S)Q}{4\pi\Lambda_S D^2 R} \theta(t), \quad (1.4)$$

$$D^2 = g \left(\frac{\chi}{k_S \Lambda_S} + \frac{1}{\Lambda_T} \right), \quad N^2 = g \left(\frac{1}{\Lambda_S} + \frac{1}{\Lambda_T} \right), \quad Q = g \frac{\alpha P}{c_p \rho_0}, \quad \delta(R) = \frac{\delta(z)\delta(r)}{2\pi r}.$$

Applying the Fourier-Bessel transform

$$F(k_r, k_z, \omega) = \frac{1}{2\pi} \int_0^{+\infty} \left\{ \int_{-\infty}^{+\infty} f(r, z, t) \exp(ik_z z - i\omega t) dt dz \right\} r J_0(k_r r) dr$$

(J_0 is the zeroth-order Bessel function of the first kind) to Eq. (1.4), finding the transform of the function $f(r, z, t)$, and taking the inverse transform, we obtain an integral representation for $f(r, z, t)$:

$$f(r, z, t) = -\frac{Q}{(2\pi)^3} \int_0^{+\infty} \left\{ \int_{-\infty}^{+\infty} \frac{(i\omega + k_S k^2) \left(\pi \delta(\omega) + i \text{Vp} \frac{1}{\omega} \right) \exp(i\omega t - ik_z z) d\omega dk_z}{k^2 (i\omega + \chi k^2) (i\omega + k_S k^2) (i\omega + \nu k^2) + k_S D^2 k^2 k_r^2 + i\omega N^2 k_r^2} \right\} k_r J_0(k_r r) dk_r. \quad (1.5)$$

Here $k^2 = k_r^2 + k_z^2$, and $\text{Vp}(1/\omega)$ is a function in the principal-value sense, whose properties are given by the relation

$$\int_{-\infty}^{+\infty} \varphi(\omega) \text{Vp} \frac{1}{\omega} d\omega = \lim_{\varepsilon \rightarrow +0} \left(\int_{-\infty}^{-\varepsilon} \frac{\varphi(\omega)}{\omega} d\omega + \int_{\varepsilon}^{+\infty} \frac{\varphi(\omega)}{\omega} d\omega \right).$$

The representation (1.5) decomposes into two parts:

$$f_{\text{st}} = -\frac{Q}{(2\pi)^2} \int_0^{+\infty} \left\{ \int_{-\infty}^{+\infty} \frac{\exp(-ik_z z) dk_z}{\nu \chi k^6 + D^2 k_r^2} \right\} k_r J_0(k_r r) dk_r; \quad (1.6a)$$

$$f_{\text{tr}} = -\frac{Q}{(2\pi)^2} \int_0^{+\infty} \left\{ \int_{-\infty}^{+\infty} [F_1(k_r, k_z) \exp(-a_1 t) + F_2(k_r, k_z) \exp(-a_2 t) + F_3(k_r, k_z) \exp(-a_3 t)] \exp(-ik_z z) dk_z \right\} k_r J_0(k_r r) dk_r \quad (1.6b)$$

$$(a_i = a_i(k_r, k_z), \text{Re} a_i > 0).$$

The explicit forms of the functions $F_i(k_r, k_z)$ and $a_i(k_r, k_z)$ are too cumbersome to give here. The first part is time-invariant and describes DGWs, while the second part is time-dependent and describes both the transient process in the formation of DGWs [of course, with allowance for Eq. (1.6a)] and the structure of the associated unsteady flows.

At the initial times, both steady and unsteady flows exist at a fixed point of space at a finite distance from the source. After a certain time interval has elapsed, the oscillations described by Eq. (1.6b) die out, and the flow is described by relation (1.6a) alone.

2. Structure of Dissipation-Gravity Waves. To find the DGW velocity field, we analyze the asymptotic behavior of f_{st} at large distances from the heat source along a designated direction, which is characterized by the quantities γ (tangent of the angle relative to the horizontal) and R (distance from the source).

The steepest-descent method [14] and the representation (1.3) give estimates of the radial and vertical components of the velocity u at $R \gg (2\nu\chi/D^2)^{1/4}$:

$$\begin{aligned}
u_r &\sim U(\gamma, R) \sin \left\{ \left(\frac{D^2(1+\gamma^2)}{4\nu\chi} \right)^{1/4} R - \pi/4 \right\}, \\
u_z &\sim -\gamma U(\gamma, R) \cos \left\{ \left(\frac{D^2(1+\gamma^2)}{4\nu\chi} \right)^{1/4} R - \pi/4 \right\}, \\
U(\gamma, R) &= \frac{\gamma Q}{8\pi D (\nu\chi)^{1/2} R} \exp \left\{ - \left(\frac{D^2(1+\gamma^2)}{4\nu\chi} \right)^{1/4} R \right\}.
\end{aligned} \tag{2.1}$$

The DGWs generated by the potential part of the velocity are described entirely by the first term for h in Eq. (1.4). The resulting cumbersome expression is not written out, since the ratio between the potential and solenoidal parts of the DGW velocity is proportional to $(\chi\nu N^2/gD^2)(D^2/4\nu\chi)^{3/4} \ll 1$ in the asymptotic region, and the contribution of the function h can be disregarded.

Equations (2.1) describe waves with a time-invariant velocity field. It follows from Eq. (2.1) that the nature of these waves is determined by the combined influence of dissipative processes (as attested by the existence of the coefficients χ , ν , and kg in the representation of the velocity field) and buoyancy forces (coefficients D^2 and N^2). For this reason, the term "dissipation-gravity" waves is better suited to such waves than the term "zero-frequency" waves [1-3], because it more accurately reflects their essential nature. It is also evident from Eq. (2.1) that a DGW is characterized by a wavelength

$$\lambda = 2\pi \left(\frac{4\nu\chi}{D^2(1+\gamma^2)} \right)^{1/4}, \tag{2.2}$$

and the magnitude of the energy flux density vector $\mathbf{q} = \rho \mathbf{u}(u^2/2 + c_V T + p/\rho)$ reaches a maximum at values of γ close to zero, dictating the almost horizontal propagation of these waves at large distances from the source.

It is important to investigate the paths of particles involved in dissipation-gravity oscillations. Following Sretenskii [15], we write the dynamical equations for the fluid medium, making use of Eqs. (2.1):

$$\begin{aligned}
\frac{dr}{dt} &= \frac{\gamma A}{\sqrt{r^2+z^2}} \exp \{ -B\sqrt{r^2+z^2} \} \sin(-B\sqrt{r^2+z^2} - \pi/4 - \omega t), \\
\frac{dz}{dt} &= -\frac{\gamma^2 A}{\sqrt{r^2+z^2}} \exp \{ -B\sqrt{r^2+z^2} \} \cos(-B\sqrt{r^2+z^2} - \pi/4 - \omega t).
\end{aligned} \tag{2.3}$$

Here

$$A = \frac{Q}{8\pi D (\nu\chi)^{1/2}}; \quad B = \left(\frac{D^2(1+\gamma^2)}{4\nu\chi} \right)^{1/4},$$

and the substitution $R^2 = r^2 + z^2$ has been made. The integration in Eq. (2.3) is carried out on the basis of the series expansion of r and z in powers of the parameter γ :

$$\begin{aligned}
r &= r_0(t) + \gamma^{1/2} r_1(t) + \gamma r_2(t) + \dots, \\
z &= z_0(t) + \gamma^{3/2} z_1(t) + \gamma^3 z_2(t) + \dots
\end{aligned} \tag{2.4}$$

The substitution of Eq. (2.4) in (2.3) and the evaluation of the zeroth- and first-order terms lead to the result

$$\begin{aligned}
r_0(t) &= \alpha, \quad z_0(t) = \beta, \\
r_1(t) &= \frac{A}{\omega \sqrt{\alpha^2 + \gamma^2 \beta^2}} \exp \{ -B\sqrt{\alpha^2 + \gamma^2 \beta^2} \} \cos(-B\sqrt{\alpha^2 + \gamma^2 \beta^2} - \\
&\quad - \pi/4 - \omega t) + C_1, \\
z_1(t) &= \frac{A}{\omega \sqrt{\alpha^2 + \gamma^2 \beta^2}} \exp \{ -B\sqrt{\alpha^2 + \gamma^2 \beta^2} \} \sin(-B\sqrt{\alpha^2 + \gamma^2 \beta^2} - \\
&\quad - \pi/4 - \omega t) + C_2,
\end{aligned} \tag{2.5}$$

where α , β , C_1 , and C_2 are constants.

The constants C_1 and C_2 are determined in such a way that α and β will be the Lagrangian coordinates of a moving liquid particle. We eventually arrive at the approximate path equations

$$\begin{aligned} r &= \alpha + \frac{A\gamma^{1/2}}{\omega\sqrt{\alpha^2 + \gamma^2\beta^2}} \exp\{-B\sqrt{\alpha^2 + \gamma^2\beta^2}\} [\cos(-B\sqrt{\alpha^2 + \gamma^2\beta^2} - \\ &\quad - \pi/4 - \omega t) - \cos(-B\sqrt{\alpha^2 + \gamma^2\beta^2} - \pi/4)], \\ z &= \beta + \frac{A\gamma^{3/2}}{\omega\sqrt{\alpha^2 + \gamma^2\beta^2}} \exp\{-B\sqrt{\alpha^2 + \gamma^2\beta^2}\} [\sin(-B\sqrt{\alpha^2 + \gamma^2\beta^2} - \\ &\quad - \pi/4 - \omega t) - \sin(-B\sqrt{\alpha^2 + \gamma^2\beta^2} - \pi/4)]. \end{aligned} \quad (2.6)$$

Passing to the limit $\omega \rightarrow 0$ in relations (2.6) and simultaneously combining the expressions for r and z , we obtain the ellipse equation $\gamma^2(r - \alpha)^2 + (z - \beta)^2 \sim [A^2\gamma^3/(\alpha^2 + \gamma^2\beta^2)] \cdot \exp\{-2B\sqrt{\alpha^2 + \gamma^2\beta^2}\}$, for which the ratio of the vertical to the horizontal semiaxis is equal to γ .

It is evident from this analysis that the theoretical and experimental results (see Fig. 1) agree. A more detailed quantitative comparison of the experimental and theoretical results requires measurements of the vertical and horizontal density gradients and flow velocity field in the DGW zone, so that additional experiments must be performed.

Equations (1.1)-(1.4) give the excess density in the form $\rho' = \rho_0(\beta S' - \alpha T') = (\nu/g)\Delta\Delta f$. In the DGW propagation zone the ratio between the vertical and horizontal excess-density gradients is proportional to $1/\gamma$, indicating the existence of almost horizontal high-gradient boundaries, as seen in Fig. 1.

Another interesting problem is the stability of DGWs against perturbations of the density distribution (initial stratification). In real media $\nu \gg \chi \gg k_S$. If the condition $\chi\Lambda_T \gg k_S\Lambda_S$ holds (as is true in a broad class of physical situations), λ varies only slightly for small and even fairly large variations of Λ_T . Since $\chi \gg k_S$, the condition $\chi\Lambda_T \gg k_S\Lambda_S$ can be satisfied when the temperature stratification scale is much smaller than the salinity stratification scale. Based on Eq. (2.2), this implies that DGWs are stable against local variations of the temperature gradients in the medium.

In real physical situations involving heat sources with above-critical power, convective motion of the medium takes place in the vicinity of the heat source (as mentioned above), so that the flow structure cannot be described by Eqs. (1.4). On the other hand, the convection zone is also bounded, and the solutions of the linearized problem are valid outside its limits, as discussed in [11] and observed experimentally in [1, 2, 6]. In subcritical flow regimes, i.e., when the power of the heat source is below critical [2], the solutions of Eqs. (1.4) are valid in all space.

It follows from the theoretical model and observations that dissipation-gravity waves are an essential element of the convective flow pattern of stratified media. They distort the initial density distribution at large distances from the source and transfer energy, momentum, and torque. The calculated DGW pattern is qualitatively consistent with the pattern observed in experiments on thermoconcentration convection in liquids with a stable salinity gradient.

LITERATURE CITED

1. V. S. Tupitsyn and Yu. D. Chashechkin, "Free convection over a point heat source in a stratified fluid," *Izv. Akad. Nauk SSSR, Mekh. Zhidk. Gaza*, No. 2 (1981).
2. Yu. D. Chashechkin and V. S. Belyaev, "Free thermoconcentration convection regimes over a point heat source," *Dokl. Akad. Nauk SSSR*, 267, No. 3 (1982).
3. Yu. D. Chashechkin and V. S. Tupitsyn, "Structure of free convective flow over a point heat source in a stratified fluid," *Dokl. Akad. Nauk SSSR*, 248, No. 5 (1979).
4. B. R. Morton, G. I. Taylor, and J. S. Turner, "Turbulent gravitational convection from maintained and instantaneous sources," *Proc. R. Soc. London, Ser. A*, 234, No. 1196 (1956).
5. J. S. Turner, *Buoyancy Effects in Fluids*, Cambridge Univ. Press (1973).

6. V. S. Belyaev and Yu. D. Chashechkin, "Free thermoconcentration convection regimes over a localized heat source," *Izv. Akad. Nauk SSSR, Mekh. Zhidk. Gaza*, No. 2 (1989).
7. B. R. Morton, "Buoyant plumes in a moist atmosphere," *J. Fluid Mech.*, 2, Part 2 (1957).
8. A. B. Tsinober, Y. Yahalom, and D. J. Shlien, "A point source of heat in a stable salinity gradient," *J. Fluid Mech.*, 135, 199 (1983).
9. D. E. Mowbray, "The use of schlieren and shadowgraph techniques in the study of flow patterns in density stratified liquids," *J. Fluid Mech.*, 27, Part 2 (1967).
10. S. N. Natreba, "Reaction of stratified rotating media to local thermal effects," *Prikl. Mat. Mekh.*, 50, No. 5 (1986).
11. A. S. Kabanov and S. N. Natreba, "Free convection from a point heat source in a stably stratified medium," *Prikl. Mat. Mekh.*, 46, No. 1 (1982).
12. *Oceanology, Physics of the Ocean, Vol. 2: Ocean Hydrodynamics* [in Russian], Nauka, Moscow (1978).
13. G. K. Batchelor, *An Introduction to Fluid Dynamics*, Cambridge Univ. Press (1973).
14. F. Olver, *Introduction to Asymptotics and Special Functions*, Academic Press, New York (1974).
15. L. N. Sretenskii, *Theory of Fluid Wave Motions* [in Russian], Nauka, Moscow (1977).

PROPAGATION OF PLANE SURFACE WAVES OVER AN UNDERWATER OBSTACLE
AND A SUBMERGED PLATE

I. V. Sturova

UDC 532.59

The investigation, in the linear formulation, of wave diffraction by bottom irregularities with shadow zones, begun in [1], is continued. A rectangular underwater obstacle with a "lid" and a rigidly clamped horizontal plate (Fig. 1) are considered.

Wave scattering by an ordinary rectangular obstacle (without a "lid") has been studied in detail, both theoretically [2-5] and experimentally [6]. In [5] it is assumed that away from the obstacle the fluid is infinitely deep. Wave scattering by a horizontal plate on a free surface was examined in [3, 7].

1. Waves are propagated in a layer of ideal incompressible liquid of depth H_1 , on the bottom of which lies a rectangular obstacle with a "lid" in the form of an infinitely thin rigid horizontal plate (Fig. 1a). This plate is located at a depth H_2 below the free surface. The length of the plate L may be greater than the base of the obstacle AB , so that on the left and right of the obstacle there are cavities of length ℓ_1 and ℓ_2 , respectively. The coordinate system is so chosen that the x axis coincides with the undisturbed level of the free surface, and the y axis is directed upwards through the left-hand end of the lid. The motion of the fluid is assumed to be potential everywhere except at the corner points.

The approaching wave travels in the direction of the positive x axis and is determined by the velocity potential $\Phi_0(x, y, t) = \varphi_0(x, y) \exp(-i\sigma t)$, where $\varphi_0 = \frac{ia g \operatorname{ch} k_1(y + H_1)}{\sigma \operatorname{ch} k_1 H_1} \exp(ik_1 x)$; a and σ are the amplitude and frequency of the wave, and g is the acceleration of gravity; the wave number k_1 is determined from the equation

$$\sigma^2 = g k_1 \operatorname{th} k_1 H_1. \quad (1.1)$$

Here and in what follows in all the expressions containing the factor $\exp(-i\sigma t)$ only the real part has physical significance.

We will consider steady waves and seek the velocity potential of the disturbed flow in the form $\Phi(x, y, t) = \varphi(x, y) \exp(-i\sigma t)$. In order to determine $\varphi(x, y)$ we must solve the